Radiation Force Exerted on Subwavelength Particles near a Nanoaperture

K. Okamoto and S. Kawata

Department of Applied Physics, Osaka University, 2-1 Yamada-oka, Suita, Osaka 565-0871, Japan

(Received 24 December 1998)

We report the first numerical analysis of the radiation force exerted on a subwavelength particle by an evanescent field localized near a subwavelength aperture. The radiation force is calculated by using the Maxwell stress tensor through the electric field distribution obtained with the finite-difference time-domain method. The result indicates that a particle moves towards the aperture. We found that if two particles exist the first particle is trapped and the second one is also attracted to the first one. The radiation force is found to be larger than the forces due to thermal fluctuations and to gravity.

PACS numbers: 41.20.–q, 42.25.Gy, 42.62.Be

In 1970, Ashkin *et al.* demonstrated that two counter-propagating beams of laser light can trap a dielectric sphere of a few micrometer diameter [1], and in 1986 they showed that even a single laser beam which is focused into the sphere can pull up and trap this sphere at the position of the focus point [2]. This technology has been, in particular, well applied in biophysical sciences to trap living cells [3], measure force associated with the transcription of RNA [4], move single DNA molecules in viscous flows [5], and so on.

The force exerted on a particle is given by the total change in the momentum of the incident photons due to scattering, absorption, and spontaneous emission by the sphere. If the particle is small enough, e.g., like an atom [6,7], compared with the wavelength of the incident light, the analysis is not very difficult because the distribution of the field due to the particle is negligible.

For a sphere with the size near the wavelength of the incident light, the electromagnetic field can be determined by the Mie scattering theory [8]. Recently we found that the force exerted on a dielectric layer near a prism, by illumination under the total internal reflection conditions, is a complicated function of the incident angle and the polarization of the incident light [9]. We also found experimentally that a sphere can be moved on a channel waveguide by an evanescent field [10,11].

In this Letter, we describe the photon force exerted on a subwavelength dielectric sphere near a small aperture by the interaction between the aperture and the sphere via evanescent photons. This configuration corresponds to a near field scanning optical microscope with an aperture [12] or a scattering probe [13,14].

Figure 1 shows the model which we used to perform our numerical analysis. The surface of a glass substrate ($\varepsilon = 2.28$) is coated with a metallic layer which is assumed to be a perfect conductor in calculation, and which is in contact with water ($\varepsilon_1 = 1.77$). A circular aperture is made into this metallic layer, the diameter of which is $\lambda/4$. λ is the wavelength of the incident light in vacuum. A glass sphere ($\varepsilon_2 = 2.28$), the diameter of which is $\lambda/2$, is located in water near the aperture. The thickness of the metallic layer is $\lambda/5$. The incident light is a plane wave x linearly polarized and propagating along the z axis towards the metallic layer through the glass substrate. The x, y, and z axes are introduced in Fig. 1.

We have made a series of numerical calculations to obtain the force dependence on the position of the sphere, in order to know where the sphere is finally trapped. For each calculation, the position of the sphere was changed near the aperture, and the electric field distributions (EFD) were calculated by the finite-difference time-domain (FDTD) method [15–17]. From each calculated EFD, the radiation force was obtained from the Maxwell stress tensor on the surface of the sphere.

The radiation force calculated using the Maxwell stress tensor is an electromagnetic expression of the force which is due to the conservation of momentum of the electric field. This force occurs on the boundary of two materials with different permittivity, and its direction is perpendicular to the surface of the boundary between the two mediums, while its magnitude per unit area can be

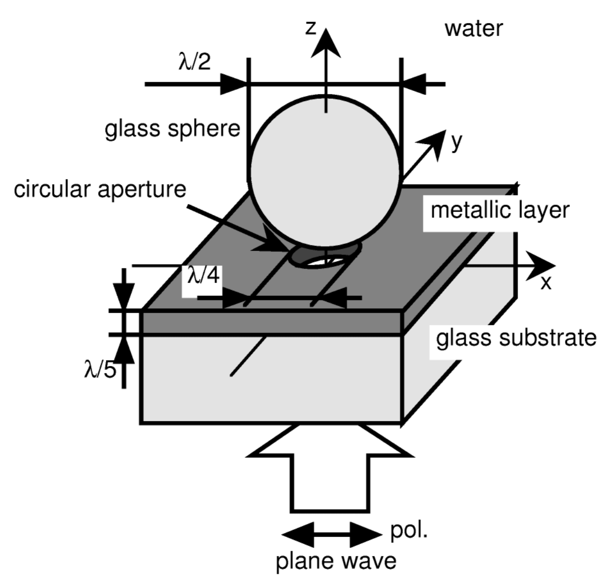

FIG. 1. The geometry of the model used for the numerical analysis. Incident light is x polarized and propagates along the z axis.

 0031-9007/99/83(22)/4534(4)$15.00

expressed as

$$F_R = \frac{\varepsilon_2 - \varepsilon_1}{2} E_p^2 + \frac{\varepsilon_1}{2} E_{s1}^2 - \frac{\varepsilon_2}{2} E_{s2}^2 . \qquad (1)$$

Equation (1) holds for a force directed from medium 2 towards medium 1, where ε_1 and ε_2 are the relative permittivity of mediums 1 and 2, respectively. E_{s1} and E_{s2} are the components of the electric fields perpendicular to the surface of mediums 1 and 2, respectively. E_p is the component of the electric field parallel to this surface. The boundary condition of the electric field imposes the same E_p for both materials. F_R is always positive when $\varepsilon_2 > \varepsilon_1$ is fulfilled. One can obtain the radiation force exerted on the sphere by integrating F_R over the whole surface of the sphere.

Figure 2 shows the calculated result of the spatial distribution of the light intensity near the aperture and the sphere. The sphere is absent in Figs. 2(a) and 2(b), and it is placed right above the aperture in Figs. 2(c) and 2(d). Figures 2(a) and 2(c) show the intensity distribution in the x-z plane, which is the plane of polarization of the incident light, and Figs. 2(b) and 2(d) show the intensity distribution in the y-z plane. In Figs. 2(c) and 2(d), it is shown that light is converged at the top of the sphere because of its lens effect. In the x-z plane, the evanescent field spreads horizontally on the upper side of the metallic surface. This is because the condition that the electric field must be perpendicular to the metallic surface is satisfied in this plane.

The arrows in Fig. 3 show how the photon force exerted on the sphere changes with the position of the sphere in the three dimensional space. The observation planes, e.g., the x-z and y-z planes, of Figs. 3(a) and 3(b) correspond to those of Figs. 2(c) and 2(d), respectively. The origin of each arrow represented by a dot in the figure corresponds to the position of the center of the sphere. Gray circles represent the sphere placed at the lowest and central positions, and correspond to the sphere in Figs. 2(c) and 2(d). In Fig. 3(a) the force near the aperture is perpendicular to the plane of aperture, and in Fig. 3(b) the force is directed towards the center of the aperture. In both the x-z and y-z planes, the sphere is attracted by the strong field near the aperture in both the horizontal, e.g., the x-y plane, and the vertical directions, e.g., z. This situation resembles the conventional optical trapping scheme in which the particle is trapped near the focus spot.

We have confirmed that this trapping effect is due to the optical near field by performing calculations with an aperture diameter equal to 2λ, so that the aperture transmits propagating light, a situation in which the near field light intensity is negligible compared to that of the far field light. Every other condition being the same as the calculations performed with an aperture size of $\lambda/4$, the result indicates that the sphere is repulsed from the aperture in the z direction, even though it is horizontally attracted towards the aperture. The difference between calculations performed with 2λ versus $\lambda/4$ aperture size is due to the difference of the initial momentum of the photons. The sphere receives an upward momentum by scattering a propagating photon, because the propagating photon initially has an upward momentum. On the contrary, evanescent photons have no upward momentum, thus the sphere receives a downward momentum by scattering an evanescent photon as a reaction of giving an upward momentum to the photon. The sphere is trapped only when the evanescent photons are dominant behind the aperture.

Figure 4 shows plots of three forces exerted on the particle, the radiation force, gravity, and the force due to

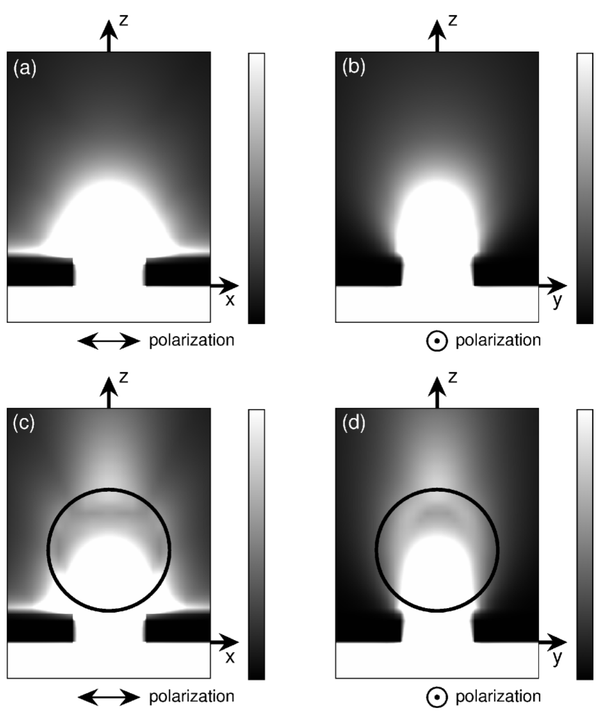

FIG. 2. Spatial distribution of the light intensity near the aperture (diameter: $\lambda/4$) and the sphere (diameter: $\lambda/2$). The dielectric sphere is absent in (a) and (b), and present in (c) and (d) (shown as a black circle). Observation planes are polarization planes of the incident for (a) and (c), and perpendicular to it for (b) and (d).

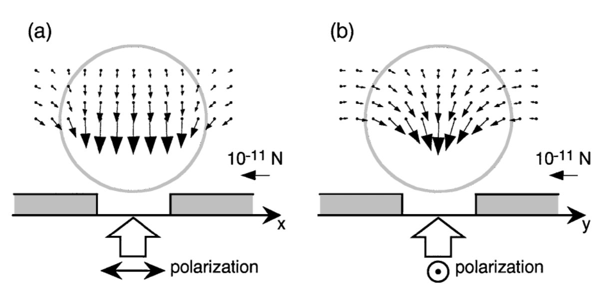

FIG. 3. Spatial distribution of photon force exerted on the sphere near a subwavelength aperture. The origin of each arrow represents the center of the sphere and vectors represent the direction and the magnitude of forces.

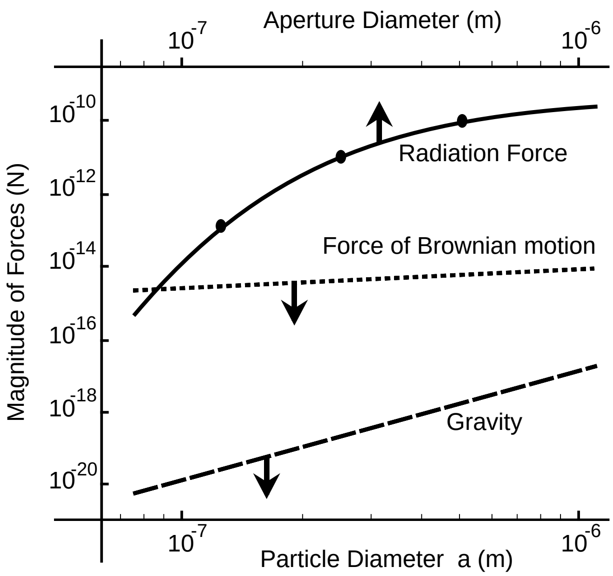

FIG. 4. Forces given to the particle in the model of Fig. 1. Radiation force is the function of the aperture diameter, while the force of Brownian motion (dotted line) and the gravity (dashed line) are the functions of the particle diameter. The radiation force with the aperture larger than 100 nm is superior to the thermal fluctuation and the gravity for particles smaller than 1 μm.

Brownian motion, as a function of the size of the particle or the aperture. The radiation force must be the dominant force among the latter forces in order to trap the particle. We regarded these three forces as effectively exerted on particles in water and compared their magnitude.

The radiation force shown as a solid line in Fig. 4 is the most dominant among the three forces when the laser intensity of the incident light is assumed to be 0.2 $W/\mu m^2$. The magnitude of the radiation force is proportional to the laser intensity. The radiation force depends on the diameter of the aperture much more than it depends on the size of the particle. The gravity including the buoyancy is shown as a dashed line in Fig. 4. The specific gravity of a glass particle is assumed to be 2.5 g/cm^3. Both the gravity and the buoyancy processes are proportional to the third power of the diameter of the particle. The Brownian force is due to the thermal fluctuations. The fluctuation-dissipation theorem of Einstein states that the Brownian force is equal to $6\pi a\eta k_b T$, where a is the diameter of the particle, η is the viscosity of water, k_b is the Boltzmann constant, and T is the temperature of water (300 K in this calculation).

By comparing the magnitude of the radiation, Brownian and gravity forces, we found that the radiation force obtained with a 100 nm aperture is equivalent to the Brownian force of a 1 μm particle. This means that we can trap a particle smaller than 1 μm with an aperture larger than 100 nm. Apertures smaller than 100 nm cannot generate sufficient radiation force to trap particles in water.

We have also investigated the radiation force with the presence of two spheres in the optical near field near a small aperture. We assumed that the first sphere is trapped near the aperture as shown in Fig. 3. Our new interest is where the second sphere is finally trapped. Both spheres are assumed to have the same refractive indices and diameters as those of Fig. 1.

Figures 5(a) and 5(b) show photon forces exerted on the second sphere in the x-z and y-z planes, respectively. Black circles represent the first sphere which does not move because it is trapped near the aperture. Gray circles indicate the highest and lowest positions of the second sphere, whose position is changed for each calculation. In both planes, the force is attractive towards the top of the first sphere. In addition, at the lowest position in Fig. 5(a), the force is strongly attractive towards the aperture. This position dependence of the force corresponds to the spatial distribution of the localized fields shown in Fig. 2. The sphere is attracted towards the strong part of the field distribution.

As a necessary check of our methodology, a comparison is made in Fig. 6 between the FDTD results and the numerical solution using the extended Lorenz-Mie theory (ELMT) [18,19] for radiation force exerted on two spheres in a plane wave. The model includes two spheres ($\varepsilon_2 = 2.28, \phi = 5\lambda$) in water ($\varepsilon_1 = 1.77$) irradiated by a linearly polarized plane wave propagating in the z direction. In this model, two spheres are arranged on the z axis, and the distance between two spheres is varied. F_1 and F_2 are the z components of the force exerted on the first sphere and the second sphere, respectively. F_1 is almost constant and F_2 varies with Δz. It is because the second sphere lies in the shadow of the first sphere against the plane wave, and hence the F_2 is strongly influenced by the electric field scattered by the first sphere. The good qualitative agreement between the results of two methods confirms the validity of the FDTD method with the two sphere system.

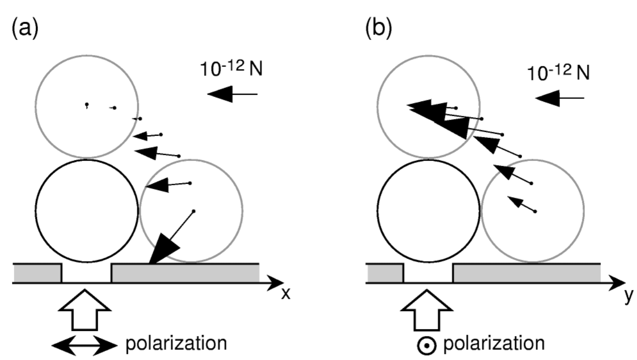

FIG. 5. The radiation force exerted on the second sphere (gray circles). Forces towards the top of the first circle (black circles) are exerted on the second sphere. In addition, at the lowest position in (a), the second sphere is strongly attracted by the evanescent field near the surface.

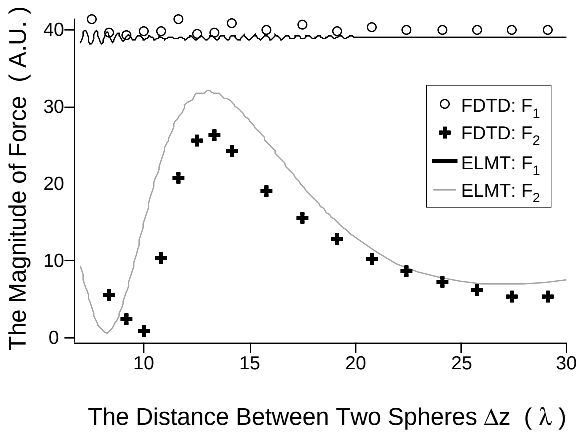

FIG. 6. Comparison of FDTD results with the numerical solutions of ELMT for the radiation force exerted on two spheres in plane wave. The horizontal axis is the distance between two spheres Δz normalized by wavelength λ in water. The first sphere (feels F_1) scatters the plane wave, and the scattered light exerts force on the second sphere (feels F_2).

We have investigated the radiation force exerted by optical near field, and found that optical trapping can be achieved. To our knowledge, this is the first investigation to confirm the possibility of optical trapping using the small aperture configuration. Besides the subwavelength aperture which we have considered, a subwavelength scatterer can also generate locally confined evanescent photons. In particular, it has been analyzed that a tip of a metallic needle can enhance the local electric field [16,17]. The magnitude of the enhanced field is sufficient to trap a particle as small as 10 nm at its tip [20]. With such an effect, the radiation force of evanescent photons can be expected to exceed the limit of the Brownian motion.

This work was supported by The Grant-in-Aid for Scientific Research on Priority Areas "Near-field Nano-optics" from the Ministry of Education, Science, Sports and Culture, Japan. We are grateful to Dr. Sugiura for his valuable discussions and suggestions.

[1] A. Ashkin, Phys. Rev. Lett. **24**, 156 (1970).
[2] A. Ashkin, J.M. Dziedzic, J.E. Bjorkholm, and S. Chu, Opt. Lett. **11**, 288 (1986).
[3] Y. Liu, G.J. Sonek, M.W. Berns, and B.J. Tromberg, Biophys. J. **71**, 2158 (1996).
[4] Hong Yin, M.D. Wang, K. Svoboda, R. Landick, S.M. Block, and J. Gelles, Science **270**, 1653 (1995).
[5] T.T. Perkins, D.E. Smith, R.G. Larson, and S. Chu, Science **268**, 83 (1990).
[6] V.I. Balykin, V.S. Letokhov, Yu.B. Ovchinnikov, and A.I. Sidorov, Phys. Rev. Lett. **60**, 2137 (1988).
[7] M.A. Kasevich, D.S. Weiss, and S. Chu, Opt. Lett. **15**, 607 (1990).
[8] M. Born and E. Wolf, *Principles of Optics* (Pergamon, Oxford, 1993), 6th ed., p. 633.
[9] T. Sugiura and S. Kawata, Bioimaging **1**, 1 (1993).
[10] S. Kawata and T. Sugiura, Opt. Lett. **17**, 772 (1992).
[11] S. Kawata and T. Tani, Opt. Lett. **21**, 1768 (1996).
[12] E.A. Ash and G. Nicholls, Nature (London) **237**, 510 (1972).
[13] T. Sugiura, T. Okada, Y. Inouye, O. Nakamura, and S. Kawata, Opt. Lett. **22**, 1663 (1997).
[14] K. Sasaki, H. Fujiwara, and M. Masuhara, J. Vac. Sci. Technol. B **15**, 2786 (1997).
[15] K.S. Yee, IEEE Trans. Antennas Propag. **14**, 302 (1966).
[16] H. Furukawa and S. Kawata, Opt. Commun. **132**, 170 (1996).
[17] H. Furukawa and S. Kawata, Opt. Commun. **148**, 221 (1998).
[18] J.P. Barton, D.R. Alexander, and S.A. Schaub, J. Appl. Phys. **65**, 2900 (1989).
[19] J.P. Barton, D.R. Alexander, and S.A. Schaub, J. Appl. Phys. **66**, 4594 (1989).
[20] L. Novotny, R.X. Bian, and X.S. Xie, Phys. Rev. Lett. **79**, 645 (1997).